

Electronic Supporting Information

**Heat triggered molecular restructuring responses the triple gel-gel-gel transformations in a Li<sup>+</sup>-integrated metallogel**

Moupia Mukherjee,<sup>a</sup> Manish Kumar Dixit,<sup>a</sup> Yeeshu Kumar,<sup>a</sup> Abul Kalam<sup>b</sup> and Mrigendra Dubey<sup>\*a</sup>

<sup>a</sup>Soft Materials Research Laboratory, Department of Metallurgy Engineering and Materials Science, Indian Institute of Technology Indore, Indore-453552, India.

<sup>b</sup>Department of Chemistry, College of Science, King Khalid University, Abha 61413, Saudi Arabia

\*Email: [mdubey@iiti.ac.in](mailto:mdubey@iiti.ac.in)

---

| Table of Contents:             | Pages |
|--------------------------------|-------|
| Materials and Physical methods | S2    |
| Synthesis and Characterization | S3    |
| Scheme S1                      | S4    |
| Figure S1                      | S5    |
| Figure S2                      | S5    |
| Figure S3                      | S5    |
| Figure S4                      | S5    |
| Table S1                       | S5    |
| Table S2                       | S5    |
| Figure S5                      | S6    |
| Table S3                       | S6    |
| Table S4                       | S7    |
| Figure S6                      | S7    |
| Figure S7                      | S8    |
| Figure S8                      | S8    |
| Figure S9                      | S9    |
| Figure S10                     | S10   |
| Figure S11                     | S10   |
| Figure S12                     | S11   |
| Figure S13                     | S11   |
| Figure S14                     | S11   |
| Figure S15                     | S12   |
| Figure S16                     | S12   |
| Figure S17                     | S13   |
| Figure S18                     | S13   |
| Figure S19                     | S14   |
| Figure S20                     | S14   |
| Table S5                       | S15   |
| Figure S21                     | S15   |
| Figure S22                     | S16   |
| Reference                      | S16   |

---

## Materials and Physical Methods:

Methanol was acquired from Avantor performance material India Ltd., Thane, Maharashtra (India). Concentrated H<sub>2</sub>SO<sub>4</sub>, DMSO, Ethanol were obtained from Qualikems Fine Chem Pvt. Ltd., Vadodara (India). All solvents were properly distilled and dried using protocol prior to use. Lithium hydroxide and Hydrazine hydrate (80%) were procured from Spectrochem Private Limited. and Sisco Research Laboratories Pvt. Ltd. (Mumbai, India). 4-(Diethylamino)salicylaldehyde was acquired from TCI Chemicals (India). Chennai (India). All the reagents were used as-received without further purification.

FT-IR data were acquired using spectrum two PerkinElmer ATR FT-IR spectrometer. Fourier Transform Nuclear Magnetic Resonance spectrometer (Model AVNACE NEO500 Ascend Bruker BioSpin International AG, Switzerland) was used to procure <sup>1</sup>H NMR spectra. UV-vis study was done on UV2600 Shimadzu spectrophotometer. PXRD data was obtained from Empyrean Malvern Panalytical instrument (Cu-K $\alpha$  radiation) between angle 2 $\theta$  = 5-80°. ESI-MS spectral analysis was carried out on Waters (Micro mass MS Technologies) Q-ToF Premier instrument and FE-SEM images were procured using JEOL-7610 F Plus. JASCO instrument (Model J-815-150S) was used to acquire CD spectra. Dry N<sub>2</sub> gas was purged (15 L.min<sup>-1</sup>) throughout the entire experiment. Quartz cuvette (l= 1 mm) was chosen for CD data acquisition (data recorded in the range of 200-400 nm). CH Instrument electrochemical workstation (model No. CHI604E) was employed to conduct Electrochemical impedance studies

## Rheological Study:

Freshly prepared metallogels **Y-TLG** (1% w/v) and **R-TLG** were subjected to rheological measurements and experiments were conducted on a Rheometer MCR 102 (Anton Paar) with the help of stainless steel parallel plates (1.0 mm gap was maintained between 25 mm diameter plates). Linear viscoelastic regions (LVE) of the metallogels were obtained in dynamic amplitude sweep experiments at constant angular frequency 10 rad.sec<sup>-1</sup>. Further, dynamic oscillatory frequency sweep was conducted between 0.1-100 rad.sec<sup>-1</sup> frequency range at constant 0.1% shear strain. Amplitude and frequency sweep experiments were conducted at 25°C for all the metallogels. Dynamic temperature ramp experiments were conducted within 25°C-100°C. Throughout the experiments, a constant 10 rad.sec<sup>-1</sup> frequency and 0.1% strain were maintained.

## Conductance Study:

Metallogels used in this experiment were synthesized *via* sonication and two different heat-cool methods which produced weak and strong gels, respectively. These freshly formulated metallogel samples and **H<sub>4</sub>TL**/LiOH solution were subjected to electrochemical impedance measurements (EIS). Experiments were carried out on an Electrochemical Workstation (model CHI604E) within the 10<sup>6</sup>-1 Hz frequency range at 0.01 V of minimal perturbation voltage. All impedance analysis were acquired at room temperature. Three electrodes set up *viz.*, Ag/AgCl reference electrode, platinum wire counter electrode and glassy carbon working electrode were used in a cylindrical electrochemical cell. The Nyquist plots obtained for metallogels were then fitted with suitable electrical circuit models with an inbuilt software provided by CHI604E instrument.

## Confocal Laser Scanning Microscopy (CLSM)

Confocal microscopic imaging for the freshly prepared **S-TLG**, **Y-TLG**, **R-TLG** metallo gels and **HY** molecule were recorded on a OLYMPUS (model- IX-83). For **S-TLG**, 40  $\mu\text{L}$  gel was pipetted out and was drop-casted on a thoroughly clean coverslip. For **S-TLG** and **Y-TLG**, the initial **H<sub>4</sub>TL**/LiOH solution was heated at first at 65 °C and then at 95 °C, respectively. 40  $\mu\text{L}$  aliquots of the heated solutions were then drop-casted on the coverslip and kept for 1 min. to form the metallo gels. Further, **HY**/Li<sup>+</sup> solution (provided similar gelation condition) was drop-casted in a similar way. The images were recorded thereafter in the gel phase. For all the three metallo gels, excitation wavelength of 405 nm and detection wavelength regions of 450-510 nm and 520-590 nm were employed.

## Synthesis and Characterization:

### Synthesis of Gelator **H<sub>4</sub>TL**:

Preparation of the precursor L-tartrac dihydrazide is mentioned in previous literature.<sup>1-3</sup> Briefly, in a round bottom flask containing methanolic solution (50 mL) of L-tartaric acid (2.00 g, 13.3 mmol) conc. H<sub>2</sub>SO<sub>4</sub> (catalytic) was charged and reflux condition was maintained for the next 15 hours. Reaction produced Dimethyl-L-tartrate as a clear oil with fruity smell and the solution was concentrated using laboratory rotatory evaporator. The resultant was then used directly for next step. Hydrazine hydrate (1.60 g, 32.00 mmol) was added drop wise to the methanolic solution of as obtained methyl L-tartrate with stirring. The resultant solution was then refluxed for 6-8 hours and further kept to cool down. Afterwards, white crystals of L-tartaric dihydrazide were obtained which were separated by filtration, washed several times with adequate amount of diethylether and dried under vacuum.

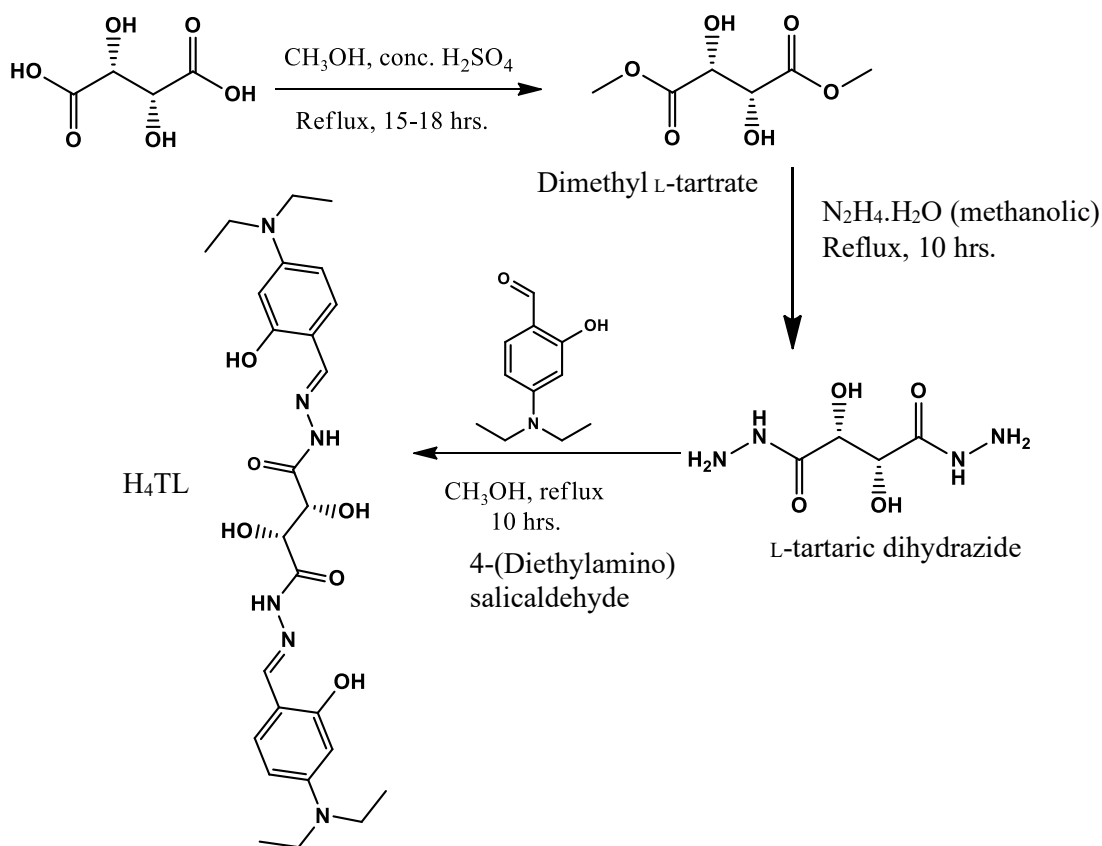
Methanolic solution of 4-(Diethylamino) salicylaldehyde (1.082 g, 5.6 mmol) was added dropwise to lukewarm aqueous solution of L-tartaric dihydrazide (0.500 g, 2.8 mmol) and stirred for 10-15 min. Further, the resulting suspension was refluxed for 7-8 hours at 55°C. This afforded pale beige-coloured solid compound and consecutively washed with methanol, diethyl ether, Dichloromethane and water. A quick wash with chloroform was served and dried in vacuum afterwards. Yield 1.064 g (72%). <sup>1</sup>H NMR (400 MHz, DMSO, ppm): 1.12 (t, 12H, CH), 3.45 (8H, CH), 4.51 (d, 2H, chiral -CH), 5.95 (s, 2H, -OH), 6.1-6.38 (4H, Ar-H), 7.2 (s, 2H, Ar-H), 8.45 (s, 2H, =CH), 11.28 (s, 2H, -NH), 12.02 (s, 2H, -OH); ESI-MS [M+H]<sup>+</sup>, 529.27 (529.27).

### Separate synthesis of **HY**:

**HY** was prepared by slightly modifying earlier reported synthesis procedure.<sup>4</sup> To a Methanolic solution of hydrazine hydrate (100 mg, 2.05 mmol), 4-(Diethylamino) salicaldehyde (795 mg, 4.10 mmol, dissolved in minimum quantity of methanol) was added dropwise. Thereafter, the mixture was refluxed for next 8 hours affording yellow coloured precipitate. The precipitate was washed with methanol (x3) and dried in vacuum. <sup>1</sup>H NMR (500 MHz, DMSO, ppm): 1.07-1.12 (t, 12H, CH), 3.45 (q, 8H, in solvent proximity), 4.51 (d, 2H, -CH), 6.0-7.1 (6H, Ar-H), 8.51 (s, 2H, =CH), 11.47 (s, 2H), ESI-MS [M+H]<sup>+</sup>: 383.2, *calc.* 383.2.

### Synthesis of metallo gels **S-TLG** and **Y-TLG**:

**H<sub>4</sub>TL** (10 mg, 0.019 mol) was dissolved in DMSO (0.20 mL) in a small 10 mL glass vial leading to clear pale-yellow solution. The fresh LiOH.H<sub>2</sub>O solution (0.002 g, 0.038 mol) in DMSO (0.8 mL) was added drop wise to the solution of gelator and was then subjected to brief sonication. The ultrasound resulted in a weak faint yellow coloured metallo gel (**S-TLG**). The **S-TLG** was then heated to 65 °C to convert it into solution and kept for cooling to room temperature. The yellow coloured metallo gel **Y-TLG** was formed upon cooling and gel phase formation was preliminarily checked by inverted vial method.



**Scheme S1:** Synthetic procedure followed to synthesize gelator **H<sub>4</sub>TL**.

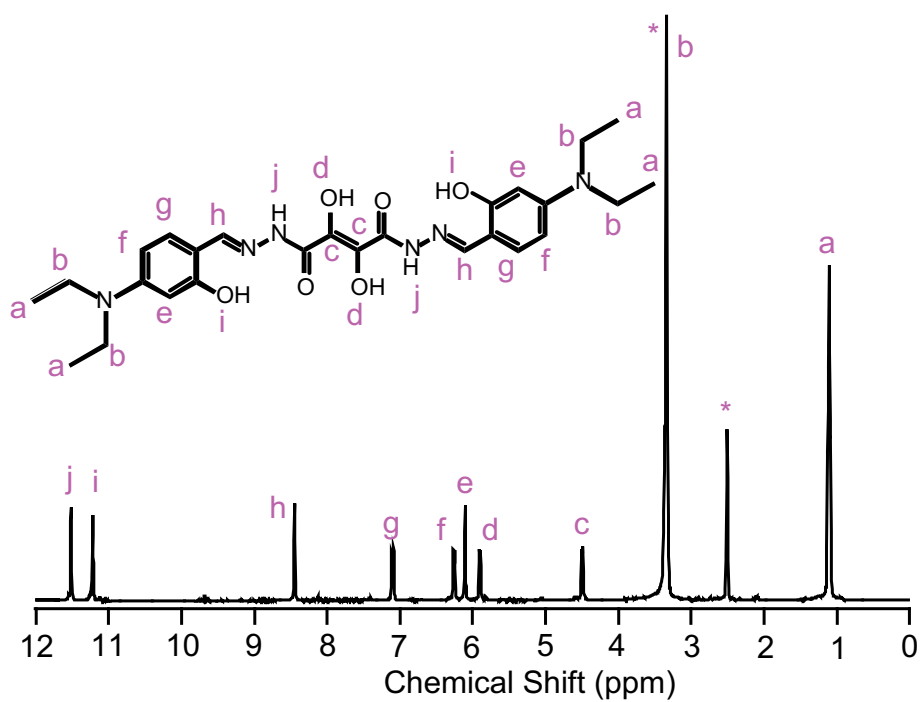


**Figure S1:**  $^1\text{H NMR}$  spectra of **H<sub>4</sub>TL** performed in  $\text{dms0-}d_6$ .

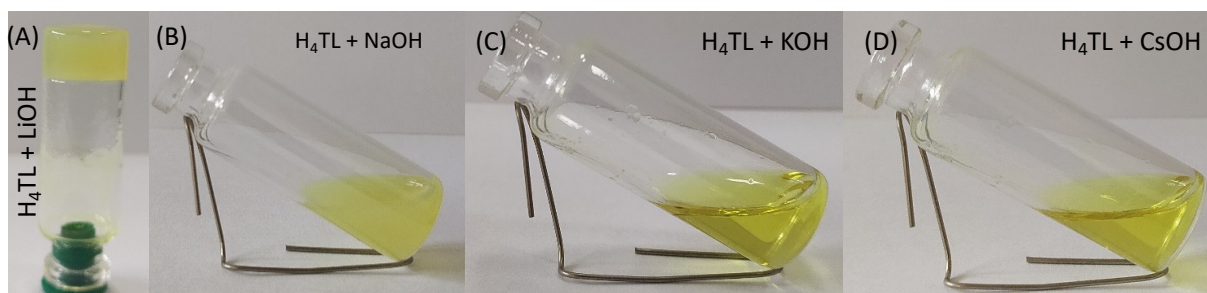


**Figure S2:** Response of  $H_4TL$  with respect to (A) LiOH, (B) NaOH, (C) KOH and (D) CsOH under similar conditions.

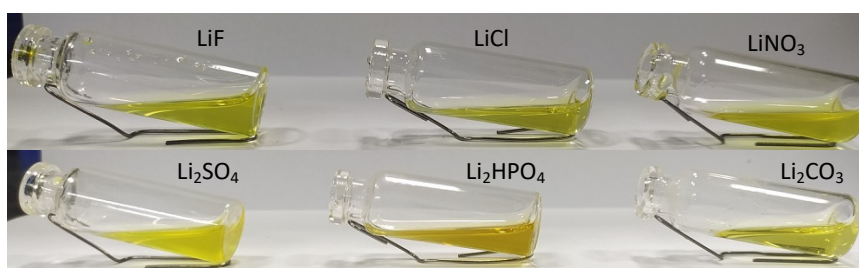


**Figure S3:** Response of  $H_4TL$  with respect to various  $Li^+$ -salts under similar conditions to gelation.

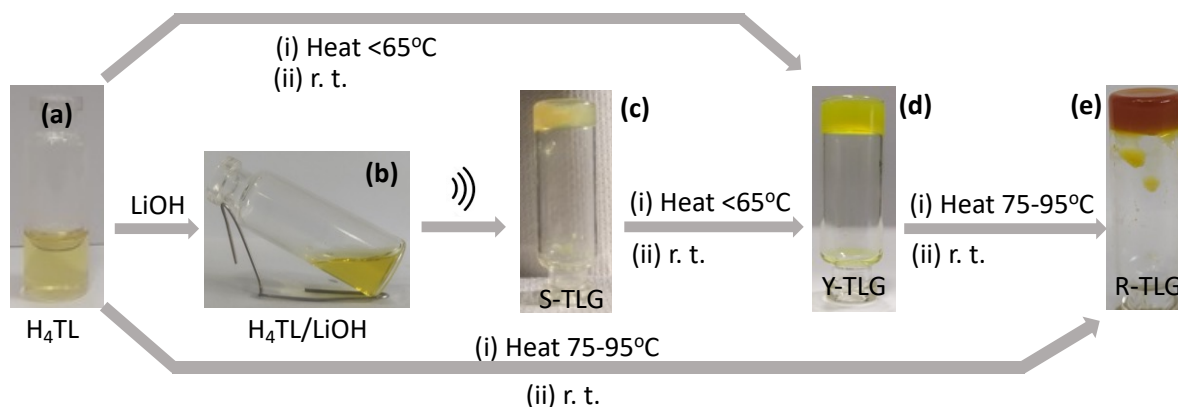


**Figure S4:** Steps involved in (a-b) **S-TLG**, (c-d) **Y-TLG** and (e-f) **R-TLG** formation.

**Table S1.** Gelation tests with respect to alkali bases.

| Solvent | $H_4TL + LiOH$ | $H_4TL + NaOH$ | $H_4TL + KOH$ | $H_4TL + CsOH$ |
|---------|----------------|----------------|---------------|----------------|
| DMSO    | G              | GP             | S             | S              |

Where, S= solution, G= gel, GP= gelatinous precipitate

**Table S2.** Gelation tests with respect to LiOH and solvent

| S. No. | Solvent    | Solubility of $H_4TL$ | Gelation Property ( $H_4TL + LiOH$ ) |
|--------|------------|-----------------------|--------------------------------------|
| 1.     | DMSO       | S                     | G                                    |
| 2.     | DMSO-water | S                     | P                                    |
| 3.     | DMF        | S                     | GP                                   |
| 4.     | Acetone    | NS                    | P                                    |

|     |              |    |     |
|-----|--------------|----|-----|
| 5.  | Acetonitrile | NS | P   |
| 6.  | Water        | NS | P   |
| 7.  | Methanol     | PS | GSP |
| 8.  | Ethanol      | NS | P   |
| 9.  | Chloroform   | PS | P   |
| 10. | DCM          | NS | P   |

Where, S= solution, G= gel, NS= not soluble, PS= partially soluble, GP= gelatinous precipitate, GSP= Gelatinous suspension.

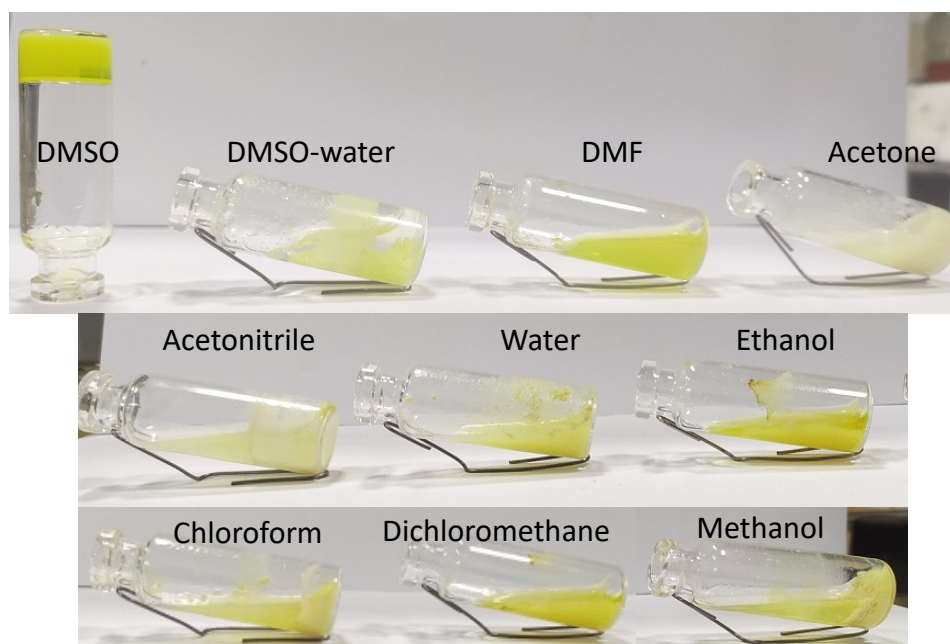


**Figure S5.** Gelation tests with respect to LiOH in presence of different solvents, as depicted in Table S2.

**Table S3:** Effect of initial weight percentage of  $H_4TL$  with 4 equivalent of LiOH over gelation time.

| S. No. | $H_4TL$ (% w/v) | Nature of mixture                    |
|--------|-----------------|--------------------------------------|
| 1.     | 0.5             | Sol                                  |
| 2.     | 0.6             | Sol                                  |
| 3.     | 0.7             | Sol                                  |
| 4.     | 0.8             | Partial gelatinous sol               |
| 5.     | 0.9             | Partial gelatinous sol               |
| 6.     | 1*              | Self-standing Gel (within 2 minutes) |
| 7.     | 2               | Gel                                  |

\*= Minimum gelation concentration determined.

**Table S4:** Gelation ability of  $H_4TL$  with increasing equivalence of LiOH.

| S. No. | $H_4TL$ (mg) | LiOH (equivalent) | Result ( $H_4TL$ + LiOH) |
|--------|--------------|-------------------|--------------------------|
| 1.     | 10*          | 1                 | Sol                      |
| 2.     | 10           | 2                 | Weak Gel                 |
| 3.     | 10           | 3                 | Weak Gel                 |
| 4.     | 10           | 4                 | Gel                      |
| 5.     | 10           | 6                 | Gelatinous suspension    |

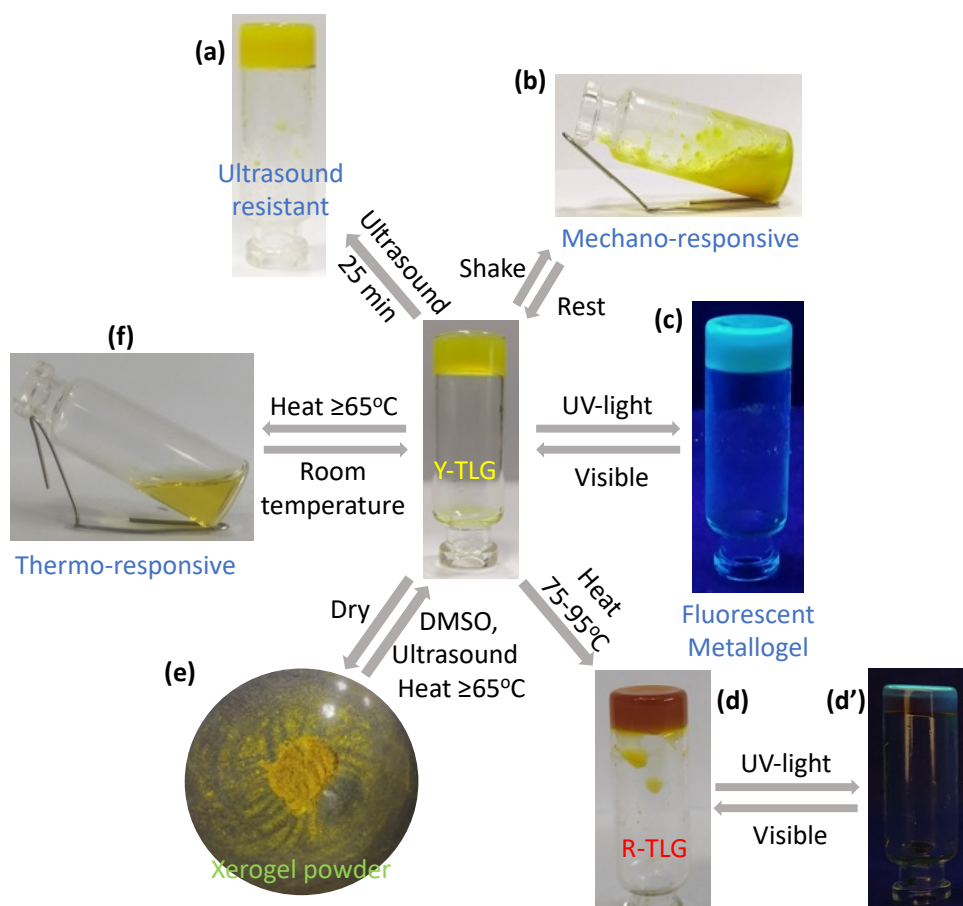


**Figure S6:** Metallogel (Y-TLG) was found to be (a) ultrasound resistant and (b) mechanoresponsive, (c) response under UV-light, (d) Thermal response of metallogel in the heating range of 65-95°C, (d') R-TLG under UV light (e) reswelling behaviour of metallogel, (f) thermo-responsive behaviour of metallogel upon heating nearly up to 65°C.

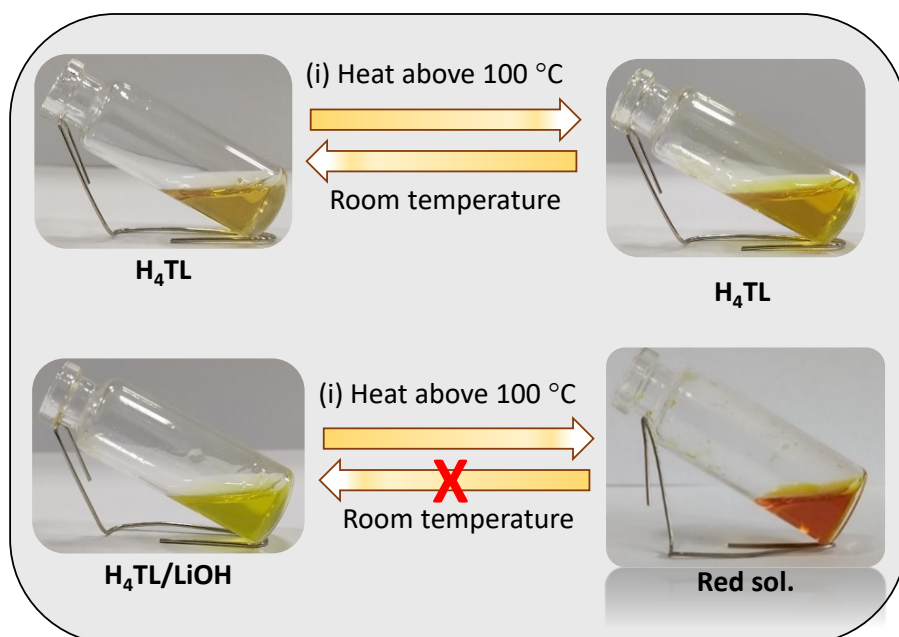


**Figure S7:** (A) No visible colour change upon heating the gelator  $H_4TL$  without LiOH even above 100°C while (B) Drastic irreversible colour change from yellow to red of  $H_4TL/LiOH$  solution, conferring essential role of basic medium in colour change.

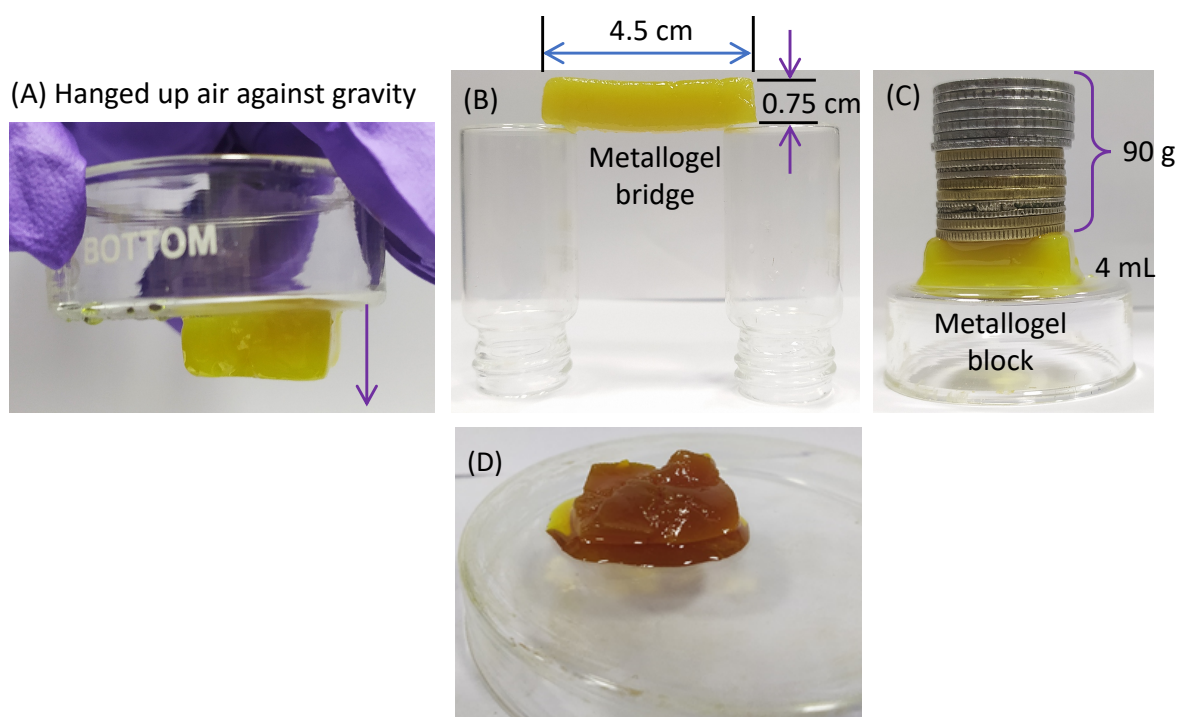


**Figure S8:** Pictures of freshly formulated  $Y-TLG$  (1% w/v) as (A) a free-standing metallogel block against gravity presenting the partial adhesive property of metallogel, (B) Metallogel can be converted in to 4.5 cm x 0.75cm block which was able to maintain a bridge like shape supported by two glass vials, and (C) A 4 ml  $Y-TLG$  block can bear up to 90 g load without its shape deformation, (D)  $R-TLG$  could not show self-standing ability.



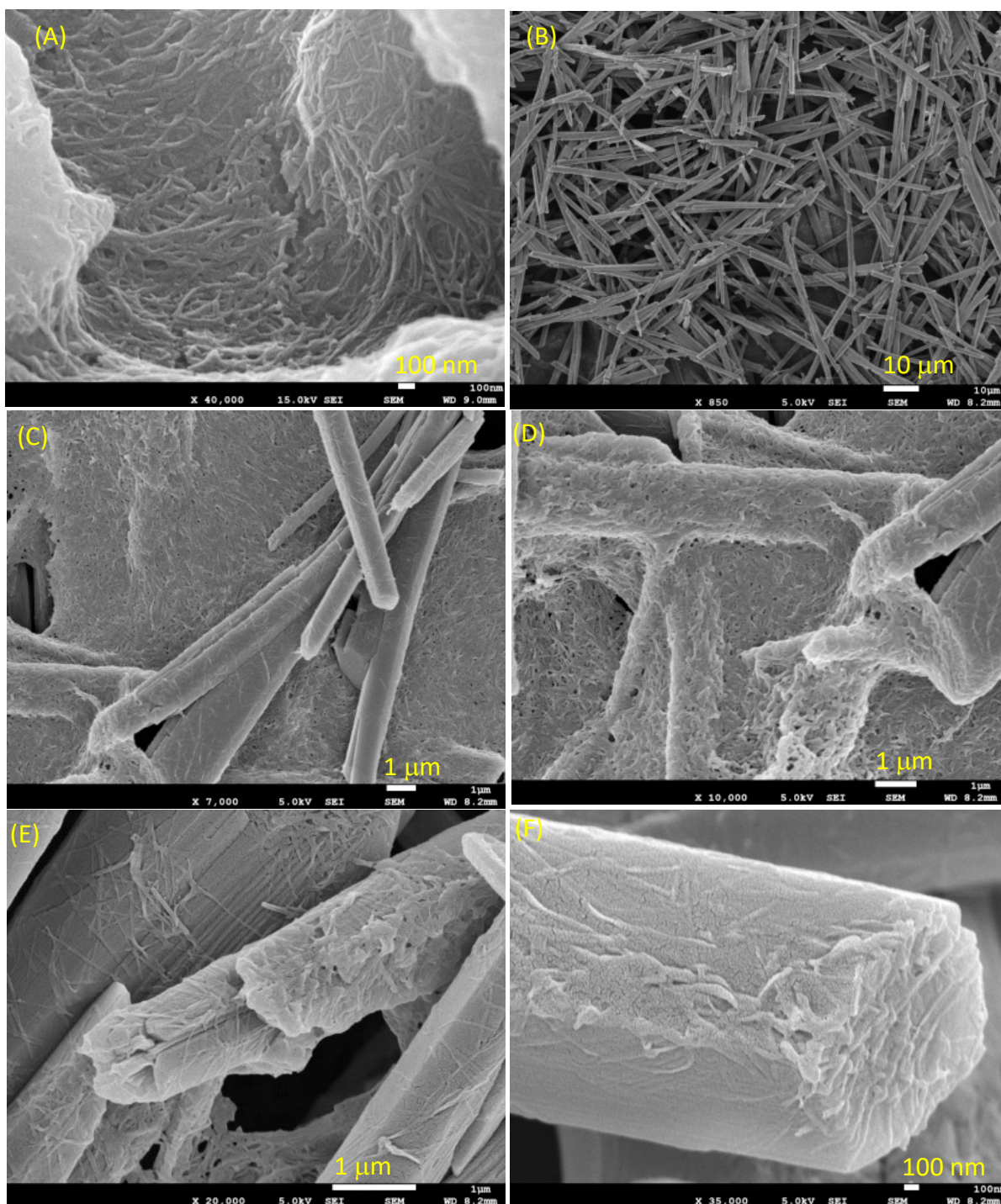


**Figure S9:** FE-SEM images of dried (A) S-TLG and (B-F) Y-TLG metallogels at three different magnifications.

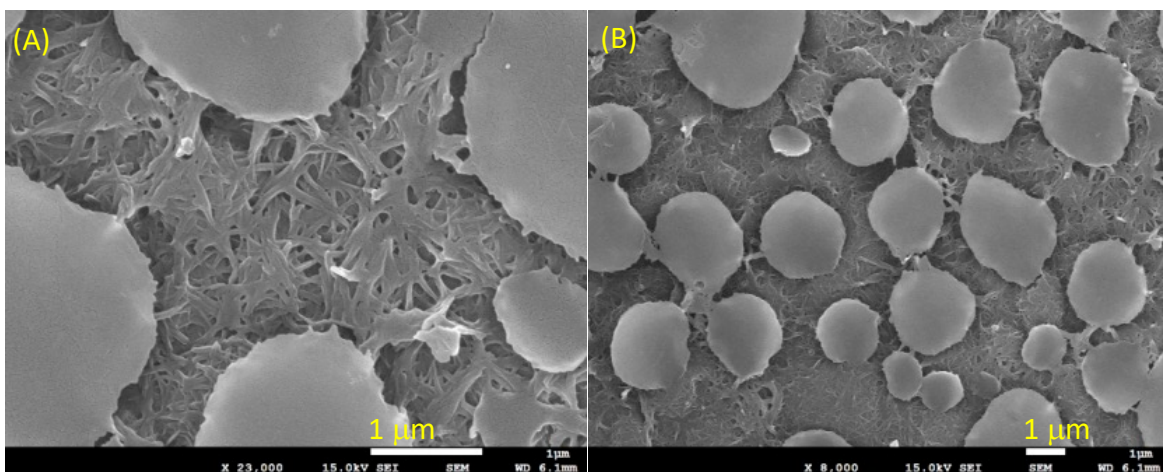


**Figure S10:** FE-SEM images of dried **R-TLG** metallogel at two different magnifications displaying comparatively thicker fibres along with lumping of fibres during heat cool cycle of 25°-95°-25°C.

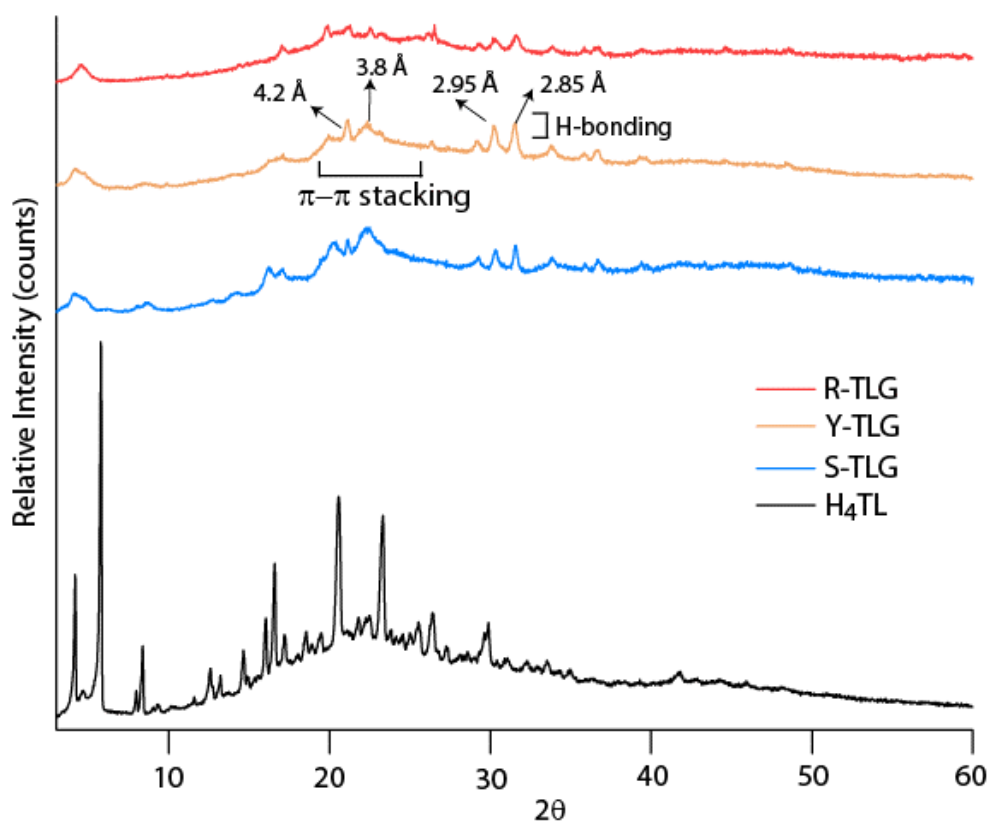


**Figure S11:** A comparative PXRD patterns of **H<sub>4</sub>TL** (red line), **S-TLG** (blue line), **Y-TLG** (orange line) and **R-TLG** (red line) xerogels.

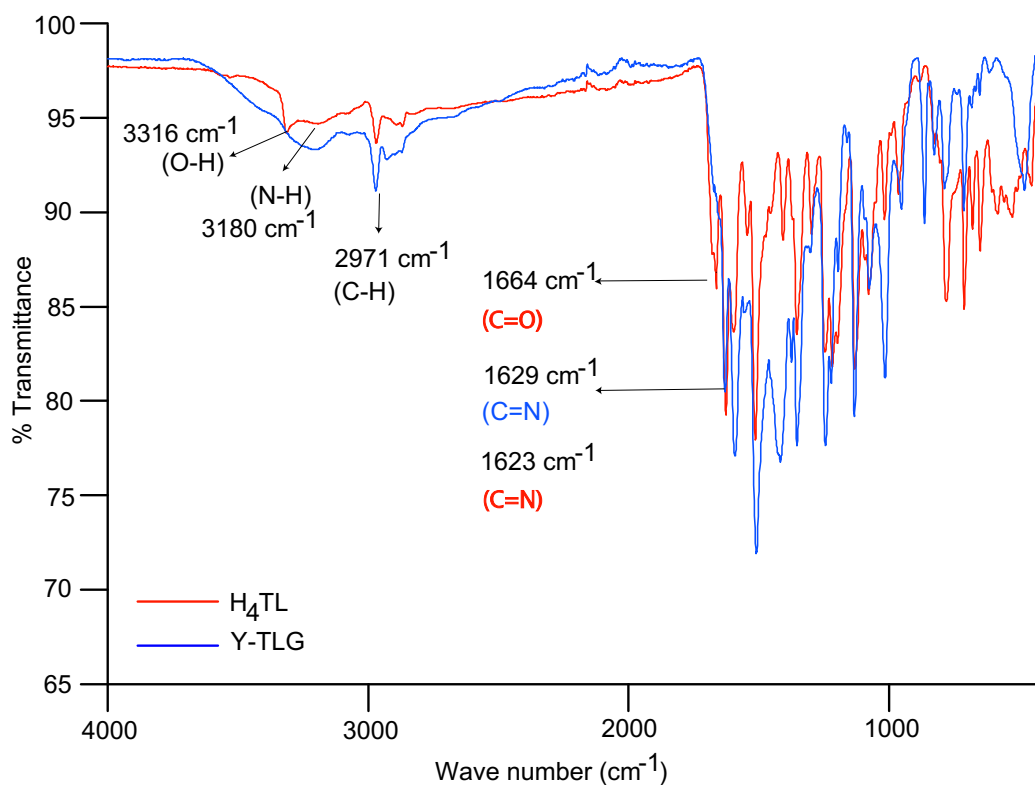


**Figure S12:** A comparative FTIR spectra of **H<sub>4</sub>TL** (red line) and **Y-TLG** xerogel (blue line).

**Note:** **Y-TLG** and **R-TLG** exhibit similar spectra pattern and hence not shown separately.

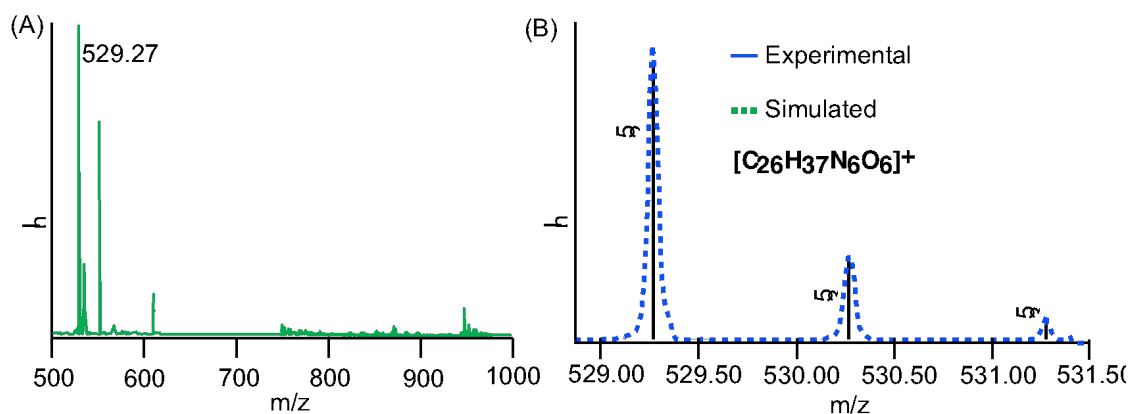


**Figure S13:** (A) ESI-MS spectra of gelator **H<sub>4</sub>TL** and (B) isotopic abundance pattern for  $m/z$  529.7 for  $[\text{C}_{26}\text{H}_{37}\text{N}_6\text{O}_6]^+$  matches nicely with simulated pattern.

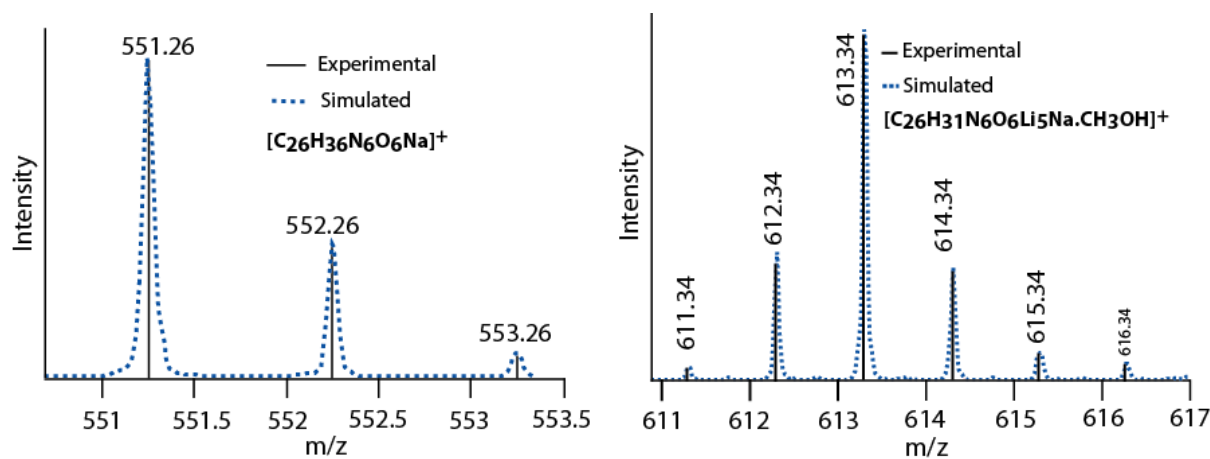


**Figure S14:** ESI-MS spectra: Isotopic abundance pattern for **Y-TLG**;  $m/z$  (left) 551.26 for  $[C_{26}H_{36}N_6O_6Na]^+$  and (right) 613.34 for  $[C_{26}H_{31}N_6O_6Li_5Na.CH_3OH]$ . The experimental pattern (black) matches with simulated (blue dotted line) pattern.

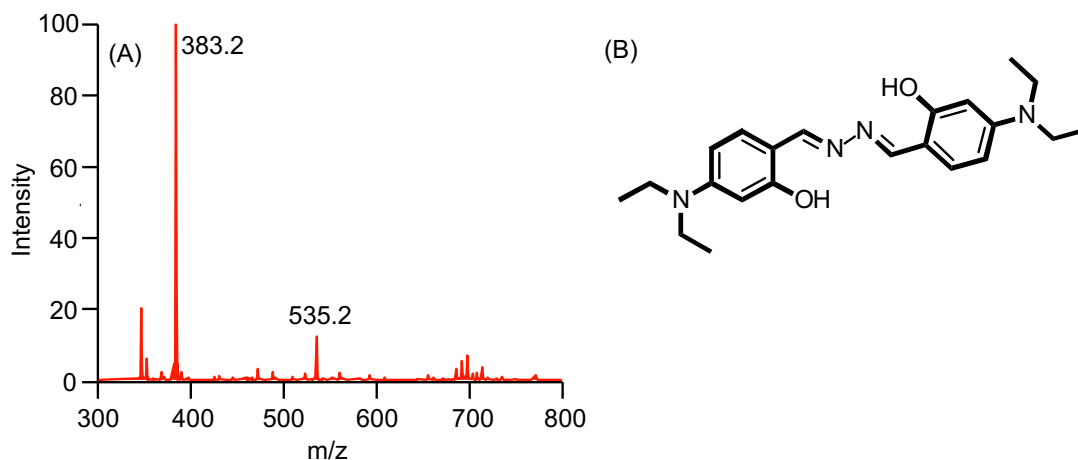


**Figure S15:** (A) ESI-MS study of the high temperature (110 °C) treated **R-Sol**, showing base peak at  $m/z$  383.2, (B) corresponding **HY** molecule, formed *via in situ* gelator dissipation and restructuring.

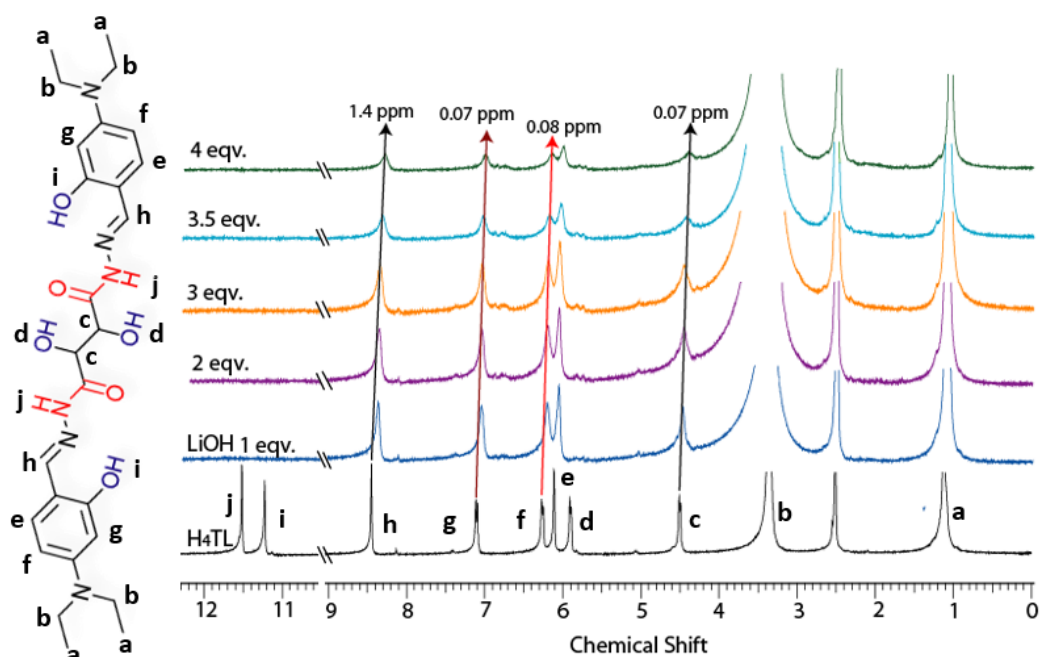


**Figure S16:**  $^1H$  NMR titration spectra of **H<sub>4</sub>TL** with 4 equiv. of LiOH ( $d_6$ -DMSO).

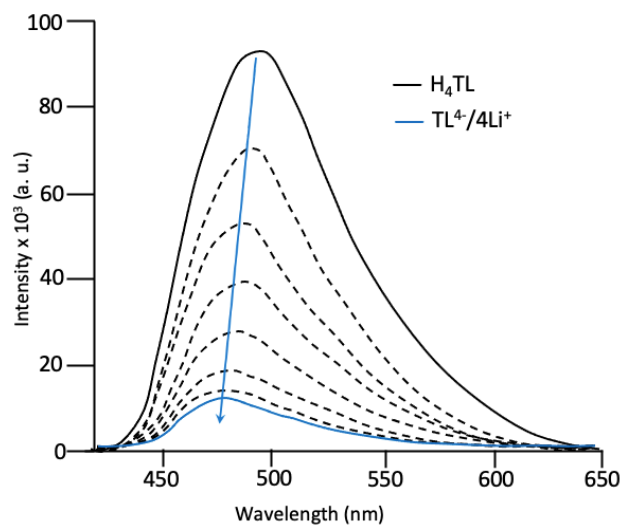


**Figure S17:** Fluorescence titration experiment of  $H_4TL$  ( $10^{-3}M$ , DMSO,  $\lambda_{ex}= 405$  nm) with 4 equivalent of  $LiOH$  ( $10^{-1}M$ , DMSO).

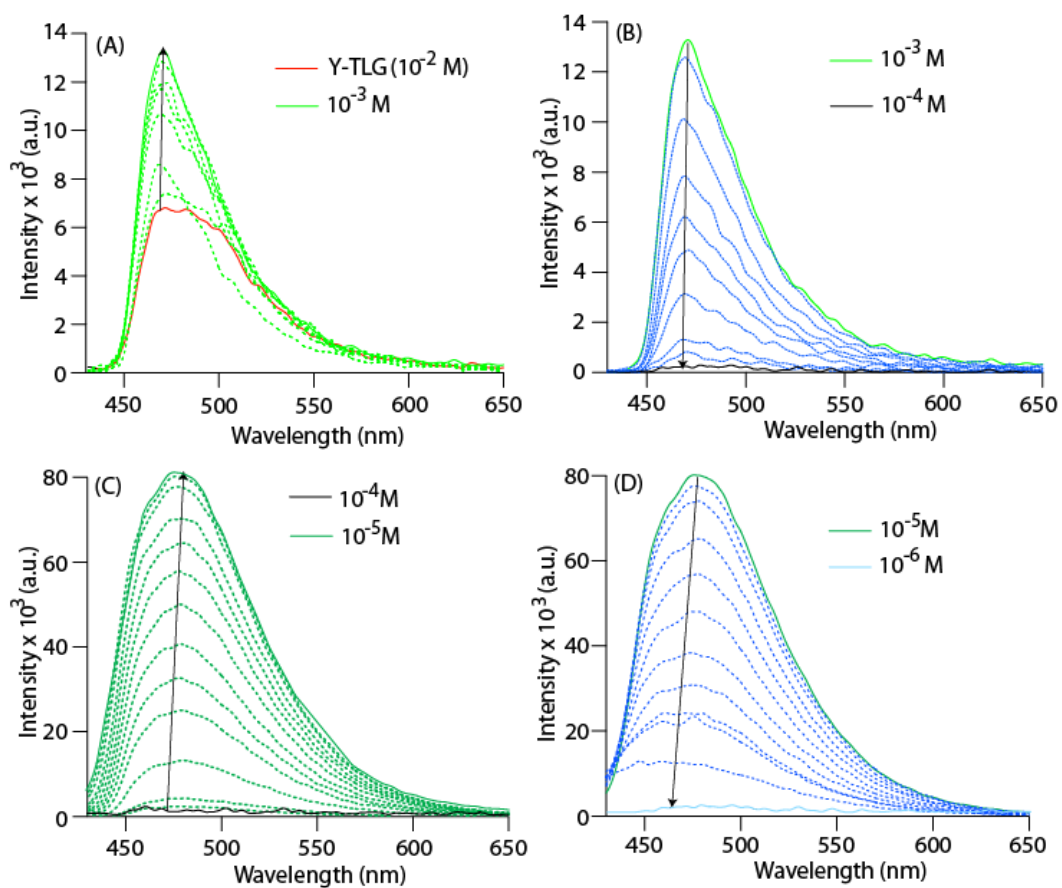


**Figure S18:** (A-D) Fluorescence dilution experiment ( $10^{-2}$ - $10^{-6}M$ ) performed over  $Y-TLG$  ( $1 \times 10^{-2} M$ ).

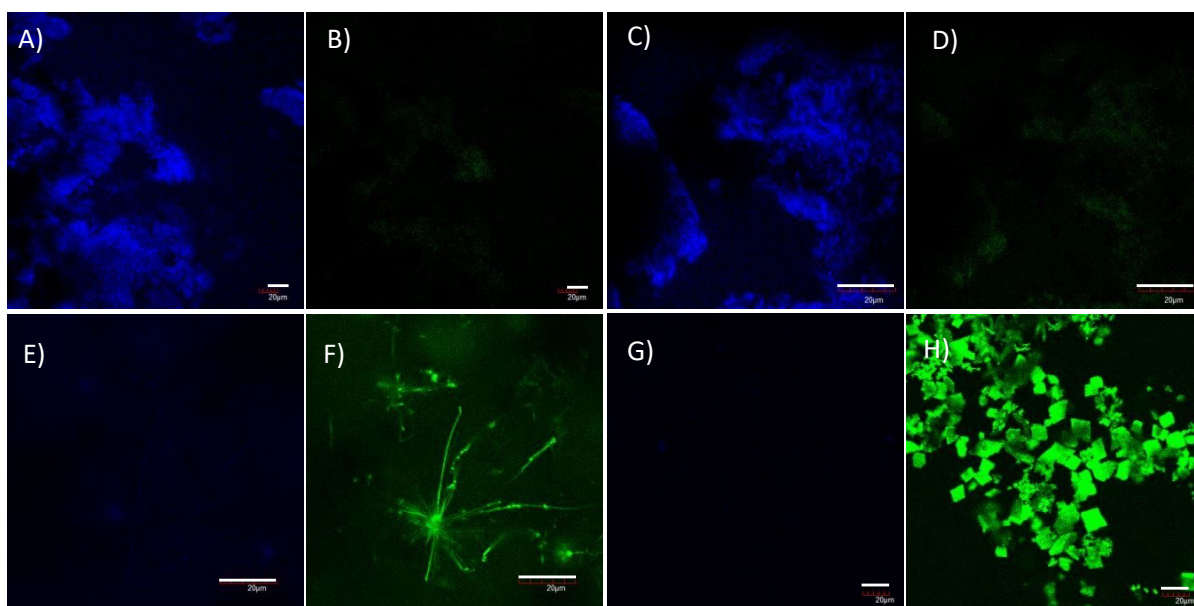


**Figure S19.** Confocal Laser scanning microscopic (CLSM) images obtained for (A, B) **S-TLG**, (C, D) **Y-TLG**, (E, F) **R-TLG**, (G, H) separately synthesized **HY/Li<sup>+</sup>** for two emission channels (430-500 nm and 510-590 nm,  $\lambda_{\text{ex}} = 405$  nm), scale bar= 20  $\mu\text{m}$ .



**Figure S20:** (A) Shape persistent ability of **H<sub>4</sub>TL-HY-Li<sup>+</sup>** metallogel (5:5; mg).

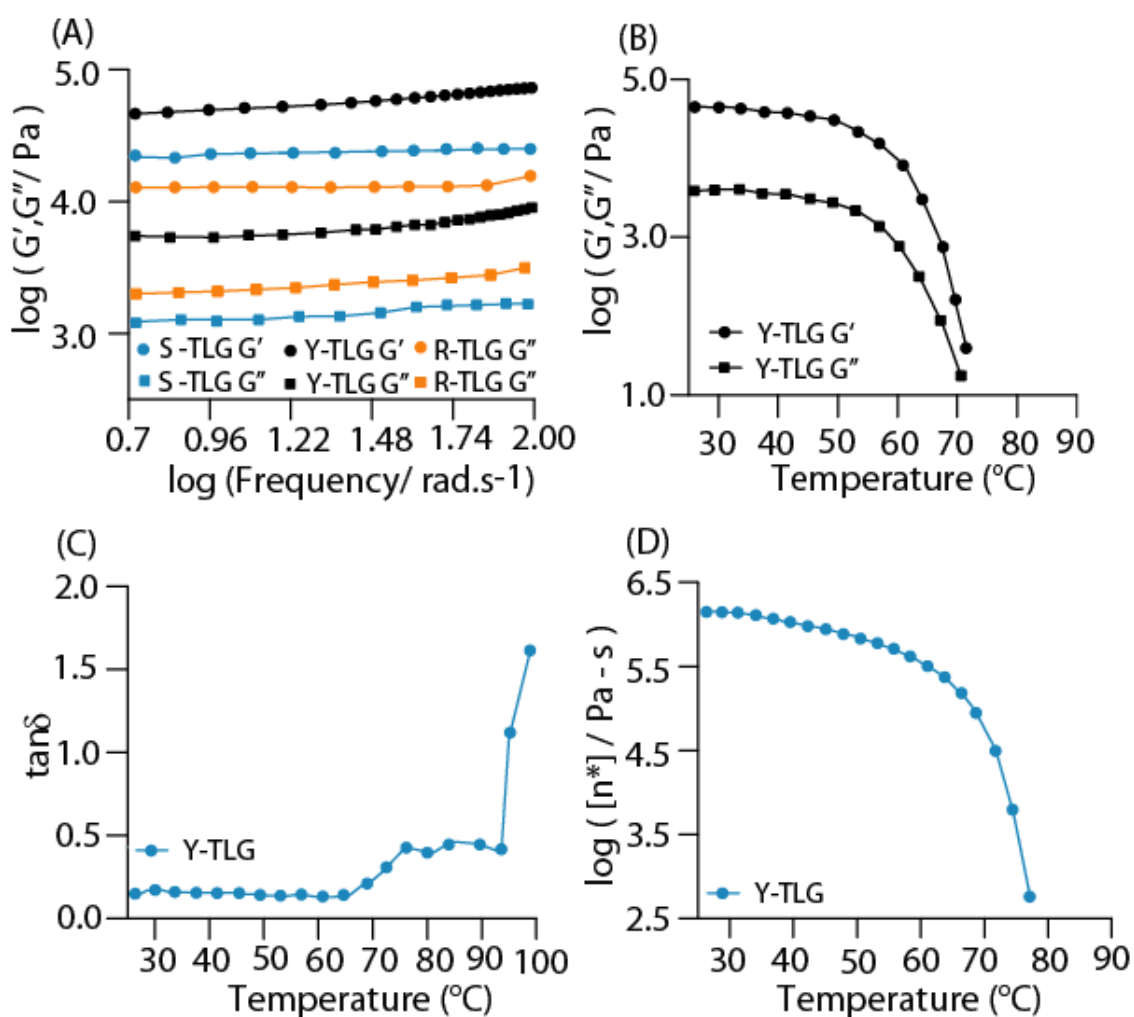


**Figure S21:** Rheological analysis of freshly formulated **S-TLG**, **Y-TLG**, **R-TLG** metallogels (1 %, w/v); (A) Dynamic frequency sweep experiment of **S-TLG**, **Y-TLG**, **R-TLG**. (B) Variation of  $G''/G'$  against temperature indicative of the gel to solution transition temperature to be  $\sim 65^{\circ}\text{C}$ , (C)  $\tan\delta$  vs. temperature plot of **Y-TLG**, and (D) Variation of complex viscosity ( $\eta^*$ ) with temperature, altogether illustrating gel-sol transition temperature.

**Table S5.**  $G'$ , yield strain and yield stress values obtained from the rheological analysis of **S-TLG**, **Y-TLG** and **R-TLG**.

|                   | <b>S-TLG</b> | <b>Y-TLG</b> | <b>R-TLG</b> |
|-------------------|--------------|--------------|--------------|
| $G'$ (Pa)         | 28000        | 44124        | 14815        |
| Yield strain (%)  | 10.12        | 2.13         | 7.76         |
| Yield stress (Pa) | 180          | 215          | 99           |

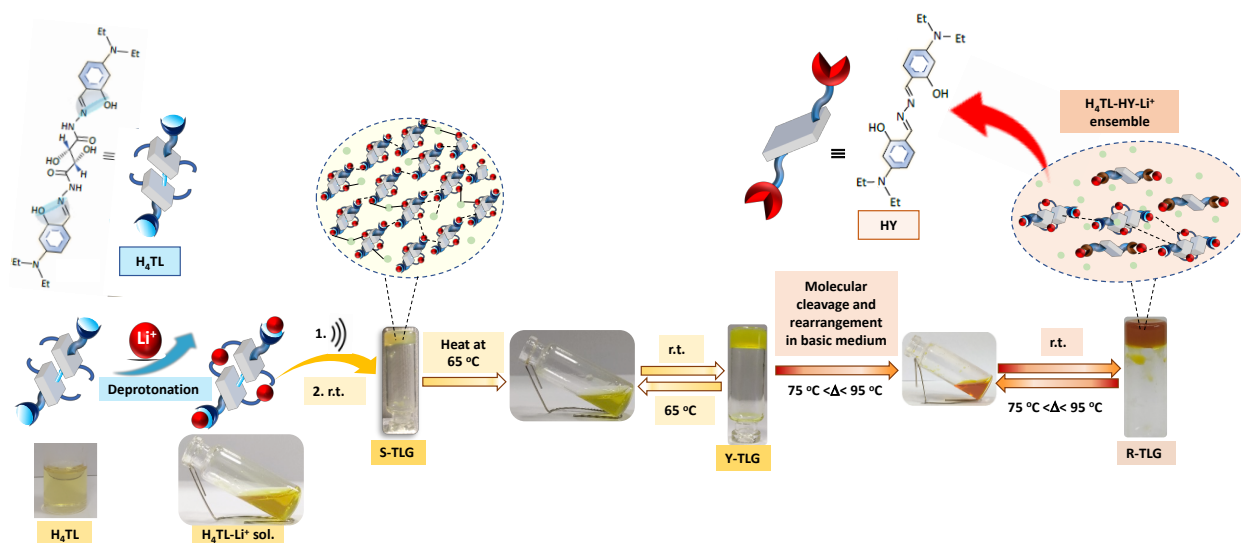


**Figure S22:** Schematic representation for steps involved during formation of **S-TLG**, **Y-TLG**, **R-TLG** under the influence of  $25\text{ }^\circ\text{C}$ ,  $25\text{-}65\text{-}25\text{ }^\circ\text{C}$  and  $25\text{-}95\text{-}25\text{ }^\circ\text{C}$  heat-cool cycles respectively.

#### Reference:

1. M. K. Dixit, V. K. Pandey and M. Dubey, *Soft Matter*, 2016, 12, 3622.
2. M. Dubey, A. Kumar, R. K. Gupta and D. S. Pandey, *Chem. Commun.*, 2014, 50, 8144.
3. C. Mahendar, M. K. Dixit, Y. Kumar and M. Dubey, *J. Mater. Chem. C*, 2020, 8, 11008.
4. F. Gou, J. Cheng, X. Zhang, G. Shen, X. Zhou and H. Xiang, *Eur. J. Inorg. Chem.*, 2016, **2016**, 4862-4866.